Co-Optimization of Energy Losses and Transformer Operating Costs Based on Smart Charging Algorithm for Plug-in Electric Vehicle Parking Lots

Seyed Soroush Karimi Madahi, Hamed Nafisi, Hossein Askarian Abyaneh, *Senior Member, IEEE*, Mousa Marzband, *Senior Member, IEEE*

***Abstract*— The global transport sector has a significant share of greenhouse gas emissions. Thus, plug-in electric vehicles (PEVs) can play a vital role in the reduction of pollution. However, high penetration of PEVs can pose severe challenges to power systems, such as an increase in energy losses and a decrease in the transformers expected life. In this paper, a new day-ahead co-optimization algorithm is proposed to reduce the unwanted effects of PEVs on the power system. The aim of the proposed algorithm is minimizing the cost of energy losses as well as transformer operating cost by the management of active and reactive powers simultaneously. Moreover, the effect of harmonics, which are produced by the charger of PEVs, are considered in the proposed algorithm. Also, the transformer operating cost is obtained from a method that contains the purchase price, loading, and losses cost of the transformer. Another advantage of the proposed algorithm is that it can improve power quality parameters, e.g., voltage and power factor of the distribution network by managing the reactive power. Afterward, the proposed algorithm is applied to a real distribution network. The results show that the proposed algorithm optimizes the daily operating cost of the distribution network efficiently. Finally, the robustness of the proposed algorithm to the number and distribution of PEVs is verified by simulation results.**

***Index Terms*— plug-in electric vehicle (PEV), transformer aging, energy losses, daily operating cost reduction.**

NOMENCLATURE

A. Indices and Sets

h	Harmonic order
h_{max}	Maximum harmonic order
N	Set of power system nodes
t	Time slot

B. Plug-in Electric Vehicle and Parking Lot Parameters

BC	PEV battery capacity [kWh]
C_p^n	Capacity of the *n*-th parking lot
D_E	Traveled distance by PEV [mile]
D_M	Maximum traveled distance by PEV [mile]
E_c	PEV electrical energy consumption [kWh/mile]
N_P	Number of parking lots
p_{loss}^{eqp}	Power loss of equipment [kW]
$S_{rated,c}$	Nominal rating of *c*-th PEV [kVA]
SOC_U/SOC_L	Upper/lower limit of SoC [%]
T_p^n	Number of PEVs appearance time steps in *n*-th parking lot
$Time_{est}^{c,n}$	Estimated staying duration for *c*-th PEV in the *n*-th parking lot [h]
$Time_{needed}^{c,n}$	Needed time for fully charging of *c*-th PEV in the *n*-th parking lot [h]
$V_{PEV,t}^{c,n}$	Inverter output voltage of *c*-th PEV at time *t* in the *n*-th parking lot [p.u.]
X_c	Reactance of *c*-th PEV coupling inductor [p.u.]

C. System Parameters

$\Delta\theta_{RHS}$	Rated winding hottest-spot temperature rise over top-oil temperature [℃]
$\Delta\theta_{RTO}$	Rated top-oil temperature rise over ambient temperature [℃]
Δt	Time interval [h]
π_t	Electricity price at time *t* [$]
$\tau_H/\tau_{mTO}/\tau_{TO}$	Winding/modified top-oil/top-oil time constant [min]
DL	Design life of transformer [year]
I_h	*h*-th harmonic order current [A]
m, n	Transformer empirical cooling values
N_t	Total number of time interval in a day
P_{EC-R}	Rated winding eddy-current loss of transformer [kW]
P_{LL-R}	Rated load loss power of transformer [kW]
P_{NLL}	No-load loss power of transformer [kW]
P_{ohm-R}	Rated DC resistance loss of transformer windings [kW]

This work was supported by the Iran National Science Foundation (INSF) under Grant 98019966. (Corresponding author: Hamed Nafisi.)

Seyed Soroush Karimi Madahi, Hamed Nafisi, and Hossein Askarian Abyaneh are with the Department of Electrical Engineering, Amirkabir University of Technology, Tehran, Iran (email: s-karimi@aut.ac.ir; nafisi@aut.ac.ir; askarian@aut.ac.ir). Mousa Marzband is with the Department: Mathematics, Physics and Electrical Engineering, Northumbria University, Newcastle, UK and with the center of research excellence in renewable energy and power systems, King Abdulaziz University, Jeddah 21589, Saudi Arabia (email: mousa.marzband@northumbria.ac.uk).

P_{OSL-R}	Rated other stray loss of transformer [kW]
Pri	Purchase price of distribution transformer [$]
r	Combined interest-inflation rate
S_{rated}^{trans}	Nameplate rating of transformer [kVA]
$S_t^{load,x}$	Load demand at time *t* and node x [kVA]
TMP_t	Ambient temperature at time t [℃]
V_U/V_L	Upper/lower limit of voltage magnitude [p.u.]
Y_{xy}/θ_{xy}	Magnitude/angle of admittance between node *x* and *y* [p.u.]

D. Variables

$\Delta\theta_{TO}^t$	Top-oil rise over the ambient temperature [℃]
$\Delta\theta_{HS}^t$	Winding hottest-spot rise over the top-oil temperature [℃]
$\Delta\theta_{UHS}^t$	Ultimate winding hottest-spot temperature rise over top-oil temperature [℃]
$\Delta\theta_{UTO}^t$	Ultimate top-oil temperature rise over ambient temperature [℃]
θ_{HS}^t	Winding hottest-spot temperature [℃]
DLC	Daily energy losses cost of the grid [$]
DOC	Daily operating cost of transformer [$]
E_t^{loss}	Energy losses of the grid at time t [kWh]
E_n^{G2V}	Total charging energy needed for the *n*-th parking lot [kWh]
F_a^{daily}	Daily aging acceleration factor of distribution transformer
F_a^t	Aging acceleration factor of distribution transformer
L_{Trans}	Transformer expected lifetime [year]
LoL	Transformer loss of life [h]
P_{EC}	Winding eddy-current loss of transformer [kW]
P_{LL}	Load loss power of transformer [kW]
P_{ohm}	DC resistance loss of transformer windings [kW]
P_{OSL}	Other stray loss of transformer [kW]
P_t^x/Q_t^x	Net injected active/reactive power at node *x* and time *t* [p.u.]
p_t^x/q_t^x	Net injected active/reactive power at node *x* and time *t* [kW/kVAR]
p_t^{trans}/q_t^{trans}	Active/reactive power of transformer at time *t* [kW/kVAR]
$pve_t^{c,n}/qve_t^{c,n}$	Active/reactive power of *c*-th PEV at time *t* in the *n*-th parking lot [kW/kVAR]
$S_t^{Parking\ lot,x}$	Demand of parking lot at time *t* and node x [kVA]
$SoC_t^{c,n}$	SoC of *c*-th PEV at time *t* in the *n*-th parking lot [%]
V_t^x/δ_t^x	Magnitude/angle of voltage at node *x* at time *t* [p.u.]

I. Introduction

Global climate change and global warming are the most critical environmental issues in the present era. The average global temperature on Earth has increased by about 0.8º Celsius since 1880, which two-thirds of it has occurred since 1975 [1]. The global CO_2 concentration has grown from 280ppm in the mid-1800s to about 400ppm in the present [2]. The global transport sector accounts for about a third of fossil fuel-based energy consumption and a quarter of greenhouse gas emissions [3]. All of the above factors and some other factors have been a motivation for the appearance, development, and usage of plug-in electric vehicles (PEVs). Plug-in hybrid electric vehicles (PHEVs) and battery electric vehicles (BEVs) are the two most popular types of PEVs. PHEVs have gotten automotive and electric power industries' attention due to the dual operation and fuel modes [4]. PHEVs have many of the benefits of BEVs without range anxiety. On the other hand, the advantages of BEVs over PHEVs are powertrain simplicity, economical bidirectional charging, and low maintenance cost. For these reasons, the combination of PHEVs and BEVs, known as PEVs, is considered in this paper. The penetration of PEVs is rapidly growing in the last years and it is expected the number of PEVs will reach 140 million in 2030 [5]. Also, PEVs can be charged at home or workplace. It was shown that only 40% of people in the US have garages in which home chargers could be installed [6].

Despite the advantages of PEVs, power systems, especially distribution networks, can be faced with some challenges due to expanding PEV numbers [7]. The uncoordinated charging of PEVs can negatively impact upon a range of power system equipment [8]. They can significantly increase the peak values and as a result, affect the electricity infrastructure [9]–[11]. Impacts of the uncoordinated charging of PEVs can be generally divided into two categories: 1) system-level impacts; 2) equipment-level impacts. The system-level impacts refer to the effects of charging PEVs on the characteristics of the distribution system. In contrast, the equipment-level impacts indicate the effects of charging PEVs on the equipment. Therefore, it is necessary to introduce a management algorithm for charging PEVs to mitigate these two undesirable effects simultaneously. Also, the management algorithm of charging PEVs can be classified into two types: 1) time coordinated charging (TCC); 2) power coordinated charging (PCC). In TCC, the number of allowed PEVs for charging at a given time is managed while in PCC, the charging power of each PEV is managed [12].

One of the system-level effects of charging PEVs is increasing energy losses and reducing the efficiency of power systems. Energy losses in this paper refer to wasteful energy caused by lines in the distribution network. Several researchers have focused on the reduction of this effect on the grid. Reference [3] has presented a two-layer method in such a way that the first layer has minimized the total daily cost of charging PEVs by active power management and the second layer has minimized the energy losses by reactive power management. The proposed method of [3] is a PCC algorithm. Article [13] has proposed the two-stage method to minimize energy losses. In this method, initially, active power has been managed globally. Next, reactive power has been managed locally. In the article, the PCC-based algorithm has been introduced. Authors in [14] have proposed a two-stage charging control strategy. In the first stage, the charging cost of PHEVs is considered as an objective. Then, in the second stage, the aggregator optimizes total losses of the network, total rescheduling costs, and wind energy utilization for charging PHEVs. The introduced method in [14] is a PCC algorithm in which PEVs can only operate in G2V mode. Article [15] has controlled PHEV storage units to reduce energy losses using a TCC-based algorithm. Among the investigated references, [14], [15] have only managed the active

power of PHEVs. Nevertheless, energy losses can be declined more when both active and reactive powers are managed. Furthermore, [13]–[15] have focused on PHEVs, while nowadays, BEVs also have a significant share of the market and both PHEVs and BEVs must be considered.

In the equipment-level point of view, transformers are one of the most expensive equipment in distribution networks. Thus, some other researchers have made an effort to mitigate the impacts of PEVs on distribution transformers. Reference [16] has developed strategies that reduce the negative impacts of PHEVs on distribution transformers. First, this paper has studied the impacts of the uncoordinated charging of PHEVs on distribution transformers. Then, to limit these negative impacts, several PCC-based strategies have been proposed and PEVs can only operate in G2V mode. Article [17] has presented a PCC-based centralized model to manage the charging of EVs from the perspective of consumers and aggregators. Consumers' perspective contains the profit of the owners of EVs, while the aggregator's perspective includes the damage cost of the transformer. Article [18] has minimized a cost function which has consisted of the energy losses, the distribution transformer aging, and a component inherent to EV. In this research, it is assumed that the charging profiles of EV battery are rectangular in a way that PEVs can only operate in G2V mode. In [18], charging EVs have been managed by a TCC-based algorithm. Moreover, PEVs pose harmonic distortions in charging points thanks to the power electronic-based chargers. In this way, harmonics affect the thermal model of transformers. None of [16]–[18] has considered the thermal model of transformers in the presence of harmonics. In addition, [16]–[18] have attempted to minimize transformer aging during charging PEVs. However, the transformer operating cost depends on both transformer aging and transformer losses. The transformer operating cost in this paper refers to the total cost of ownership over 24 hours (the daily total cost of ownership). The total cost of ownership is the sum of the initial purchase price and losses cost of the transformer for its lifetime [19]. Charging PEVs can rise the load loss of the transformer because of increasing the transformer loading. Consequently, the transformer operating cost must be optimized instead of transformer aging. Furthermore, the management of reactive power makes an impact on transformer loading while none of [16]–[18] has managed both active and reactive powers.

To the best of the authors' knowledge, none of the articles has minimized energy losses (as a system-level impact) and transformer operating costs (as an equipment-level impact) simultaneously by the management of charging PEVs. In the managed charging of PEVs, they must be charged during off-peak hours to decrease energy losses [13]. Strategies in which PEVs are charged during hours with lower ambient temperatures can optimize transformers aging efficiently [20]. In some hours during winter, there is a conflict between ambient temperature and load profile. For example, ambient temperatures are low during peak times. Thus, it is necessary to optimize energy losses as well as transformer operating costs. Besides, the management of reactive power can reduce energy losses [21] and affect transformers loading. Moreover, when PEVs operate in both grid to vehicle (G2V) and vehicle to grid (V2G) operational modes, it can decrease the energy losses [22] and transformer operating cost [17] more than when they operate only in the G2V mode. Furthermore, the mentioned publications that have concentrated on the transformer have adopted an approach to reduce transformers aging and have ignored the effect of the harmonics of PEVs charger on transformers. Nevertheless, transformer losses and harmonics play a significant role in the transformer operating cost. The mentioned references have not been able to account for all the above aspects of charging PEVs.

This paper proposes a novel day-ahead co-optimization algorithm to minimize energy losses and transformers operating costs simultaneously. Optimizing two or more different resources simultaneously is called co-optimization [23]. The objective of the paper is to propose a charging algorithm to mitigate the system-level and equipment-level effects of charging PEVs on distribution networks. This paper is the first paper which optimizes both energy losses and transformer operating costs. Furthermore, the novel PCC-based charging algorithm is proposed for parking lots in a commercial workplace. Also, the management of both active and reactive powers are conducted in the proposed algorithm. Moreover, due to the harmonic current emission of PEV charger, the effect of harmonics on transformers is modeled. In this way, for assessing transformer operating cost, the proposed algorithm employs a method that includes the installed and losses costs of the transformer. In the proposed algorithm, PEVs characteristics such as arrival and departure times and state of charge (SoC) are first gathered. Afterward, at each time of the day, the ambient temperature, transformer loading, and cost of electricity are obtained. Subsequently, the total daily operating cost is optimized by the interior point method, which is a gradient-based optimization algorithm. Ultimately, the total active and reactive power consumption of each parking lot is calculated at each time of the day. Moreover, by changing the number and distribution of PEVs, the robustness of the proposed algorithm is demonstrated.

The main contributions of this paper are according to below:

- A co-optimization algorithm to minimize energy losses (system-level), and transformers operating costs (equipment-level) is proposed;
- PEVs (a combination of PHEVs and BEVs) are considered as active and reactive powers prosumers;
- The paper develops the thermal model of transformers in the presence of harmonics;
- In this paper, an accurate method is developed for calculating transformers operating cost by considering purchase price, losses cost, and loading of transformers.

This paper is organized as follows. The motivation of the co-optimization is expressed in section II. Section III discusses the modeling of uncertain parameters. In section IV, the proposed algorithm is explained in detail. The case study and the simulation results are described in section V, and finally, section VI presents the conclusions of the paper.

II. Problem Statement

Charging PEVs during hours with lower temperature can reduce transformer operating cost. Moreover, charging PEVs when demand is low or medium can decrease energy losses. However, sometimes these objectives conflict. Fig. 1 shows the

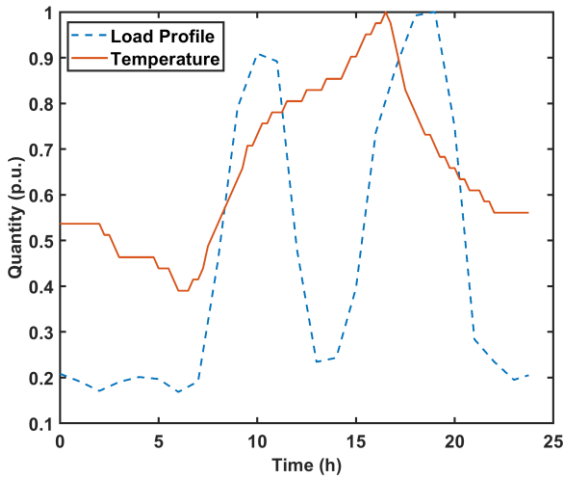

Fig. 1. The normalized temperature and commercial load profiles of a typical day in the summer in Iran.

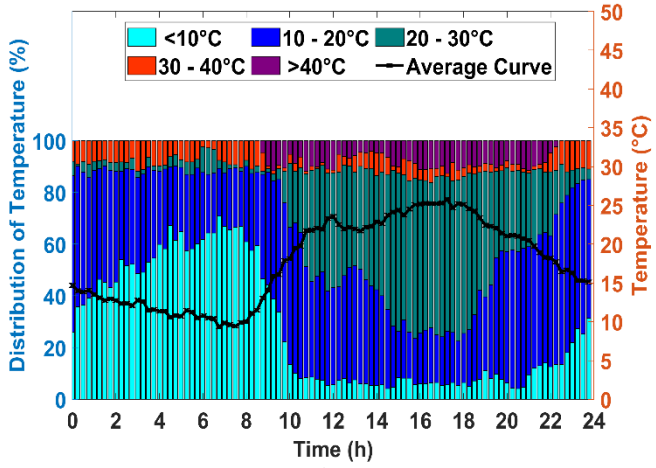

Fig. 2. Simulated ambient temperature for the spring.

normalized temperature and commercial load profiles of a typical day in the summer in Iran. According to Fig. 1, the temperature is medium and the demand is high from 9:00 am to 11:15 am and from 6:00 pm to 7:30 pm. Also, the temperature is high and the demand is very low from 12:00 pm to 3:30 pm. Therefore, it is necessary to consider both energy losses and transformer operating costs simultaneously to minimize the operating cost of the distribution network. Transformer operating cost depends on their loading, which has a relationship with both active and reactive powers of the transformer. Energy losses depend on both active and reactive powers. Thus, the management of PEVs' reactive power is as vital as the management of PEVs' active power. Unlike many previous papers, the proposed algorithm uses both active and reactive powers (in both V2G and G2V modes) to reduce the impacts of PEVs on the power grid.

III. Modeling

In this section, the stochastic and uncertain behaviors of PEVs and ambient temperature are modeled. Moreover, the thermal model of transformers is explained.

A. Ambient Temperature

As mentioned earlier, ambient temperature is one of the inputs of the proposed algorithm. In this paper, the ambient temperature is modeled stochastically using the real ambient temperature data. The spring ambient temperature data of Sirjan city, which is located in Iran, were collected. Empirical cumulative density function (ECDF) was calculated for the data in each 15-min interval. Next, 1000 sets of random numbers were generated by uniformly distributed. Then, using these sets and inverse ECDF, the sets of the simulated ambient temperature were obtained [24]. The average of these simulated sets results in the ambient temperature curve. Fig. 2 shows these simulated sets for the spring.

B. PEV Operating Curve

Transferable power and equipment ratings confine the operation of the bidirectional battery charger [13]. The mathematical model of transferable power is expressed as follows

$$(pve_t^{c,n})^2 + (qve_t^{c,n} - \frac{(V_t^x)^2}{X_c})^2 \le (\frac{V_{PEV,t}^{c,n} \times V_t^x}{X_c})^2, \qquad (1)$$

where $pve_t^{c,n}$ and $qve_t^{c,n}$ the are active and reactive powers of PEVs, respectively.

Another limitation is equipment ratings transferred power, for example, the nominal current of converter switches and outlet. This limitation can be written as

$$(pve_t^{c,n} \pm p_{loss}^{eqp})^2 + (qve_t^{c,n})^2 \le (S_{rated,c})^2. \qquad (2)$$

In this paper, it is assumed that the equipment is lossless. It is obvious from (1) and (2) that the loci of the two limitations are two circles plotted in Fig. 3. R1, which is the radius of the red circle, is equal to $\frac{V_{PEV,t}^{c,n} \times V_t^x}{X_c}$. R2, which is the radius of the green circle, is equal to $S_{rated,c}$. The red and green circles are related to the transferable power and equipment rating limitations, respectively. Fig. 3 shows that the equipment rating limits active and reactive powers exchanged between PEVs and the power system. Furthermore, Fig. 3 illustrates the operational mode of PEVs for each quadrant of the Cartesian coordinate. For example, if a PEV operates in the second quadrant of the coordinate, the PEV is in V2G mode (because of negative active power) and acts as an inductance (because of positive reactive power).

C. Arrival and Departure Times

It is assumed that the parking lots are located in commercial workplaces, which are usually active from 8:00 am to 4:00 pm. In this paper, the normal probability distribution is employed in order to model PEVs arrival and departure times. The parameters of the distributions are shown in Table I.

TABLE I
NORMAL PROBABILITY DISTRIBUTION PARAMETERS OF PEV ARRIVAL AND DEPARTURE TIMES [25]

Parameters	Arrival (h)	Departure (h)
μ	8	16
σ^2	0.1	1.2

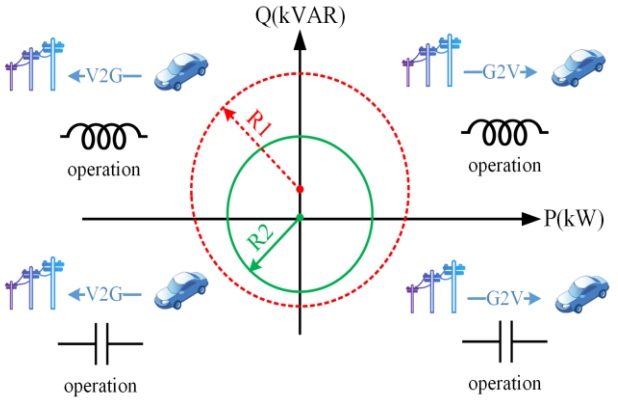

Fig. 3. PEV operating curve.

D. Daily Mileage

According to the national household travel survey (NHTS), the average annual vehicle mileage is 11,189 miles in the U.S. 58.36% of drivers drive 27 miles/day or less and 80.57% of drivers drive 41 miles/day or less [25]. Table II shows the percent of vehicles and the average annual mileage of them in each interval.

TABLE II
THE ANNUAL VEHICLE MILEAGE

Annual miles (mile)	Vehicles percent	Average (mile)
Less than 5,000	39.42%	4,239.92
5,000-9,999	18.93%	9,390.68
10,000-14,999	22.22%	13,308.27
15,000-19,999	9.39%	18,944.06
20,000-24,999	4.76%	22,114.14
25,000-29,999	1.95%	26,986.78
30,000-40,000	1.92%	35,247.93
40,000 and more	1.41%	53,018.05

E. PEV Types and Charging Level

Various types of PEVs are considered to provide a better model for the transportation fleet. In this paper, it is assumed that 50% of the whole vehicles in parking lots are PHEVs and the other are BEVs. The maximum traveled distance of PEVs (D_M) can be obtained as follows

$$BC = E_c \times D_M. \tag{3}$$

The types of PHEV40 (PHEV with D_M=40 miles) and the key parameters of each one are given in Table III [26]. BEVs can be divided into four segments according to their size. In each segment, a real reference vehicle is selected. Data of reference vehicles are extracted from [27] and the market share of each segment is mentioned in [28]. The types of BEV and the main information of them are tabulated in Table III.

In SAE J1772 standard based on voltage and power, three AC and DC charging levels are defined. In this study, it is assumed that PEVs use a single-phase connection to the grid with the maximum charging current and power 32A and 7.4kW, respectively (PEVs use AC level 2 charging).

F. State of Charge (SoC)

The percentage of remaining energy in the PEV battery is called SoC. Usually, upper and lower limits are assumed for SoC because it increases the lifetime of batteries. Using daily mileage, electrical energy consumption, and battery capacity of PEV, SoC can be calculated as

$$SOC = \begin{cases} SOC_U - \frac{E_c \times D_E}{BC} & D_E \le D_M \\ SOC_L & D_E > D_M \end{cases}. \tag{4}$$

Equation (4) indicates the SoC of a PEV after that the PEV travels D_M miles. D_M is the daily mileage of the PEV which is calculated according to section III.D. The amounts of E_c and BC for different types of vehicles are provided in section III.E and Table III. According to (4), if $D_E > D_M$, PHEVs switch to the charge sustaining mode and the internal combustion engine and electric motor work together [26] while BEVs must be immediately charged. In this paper, it is assumed that SOC_U and SOC_L are 80% and 10%, respectively.

G. Transformer Thermal Model

The aging of transformers depends on the aging of windings, bushings, and tanks. Corrosion, which is related to operating time and maintenance history, affects the aging of tanks. Thermal stress due to an overload or harmonics affects the aging of windings and bushings [29]. Therefore, the life of the transformer is not a constant value and depends on the transformer loading. For this reason, it is vital to use a method to estimate the lifetime of transformers according to present operating conditions. Transformers, which are used in this paper, are mineral-oil-immersed type transformers. The IEEE standard C57.91 has presented a model for the calculation of transformers aging [30].

Charging PEVs can affect the transformer operating cost in two ways: 1) overload transformer; 2) injecting harmonic current. Appearing PEVs in distribution networks increases the demand for active power. This growing demand may cause an overload in transformers. Moreover, the charger of PEVs injects harmonics to transformers and gains the losses of transformers. Transformer losses are classified as a no-load loss (excitation loss) and load loss (impedance loss). No-load loss is almost constant, while load loss depends on the loading of the transformer. Load loss is calculated as

$$P_{LL} = P_{ohm} + P_{EC} + P_{OSL}. \tag{5}$$

The effect of harmonics on each part of transformer load loss can be formulated as below [31]

$$P_{ohm} = P_{ohm-R} \times \left(\frac{(p_t^{trans})^2 + (q_t^{trans})^2}{(S_{rated}^{trans})^2}\right) \times \sum_{h=1}^{h_{max}} \left(\frac{I_h}{I_1}\right)^2, \tag{6}$$

$$P_{EC} = P_{EC-R} \times \left(\frac{(p_t^{trans})^2 + (q_t^{trans})^2}{(S_{rated}^{trans})^2}\right) \times \sum_{h=1}^{h_{max}} \left(\frac{I_h}{I_1}\right)^2 \times h^2, \tag{7}$$

$$P_{OSL} = P_{OSL-R} \left(\frac{(p_t^{trans})^2 + (q_t^{trans})^2}{(S_{rated}^{trans})^2}\right) \times \sum_{h=1}^{h_{max}} \left(\frac{I_h}{I_1}\right)^2 \times h^{0.8}. \tag{8}$$

TABLE III
VARIOUS TYPES OF PEV AND KEY PARAMETERS OF THEM

Type	Segment	Vehicle	Penetration level	E_c (kWh/mile)	BC (kWh)
PHEV	1	Compact sedan	20%	0.26	10.4
	2	Mid-size sedan	30%	0.3	12
	3	Mid-size SUV	30%	0.38	15.2
	4	Full-size SUV	20%	0.46	18.4
BEV	A/B (small vehicles)	BMW i3 120 Ah	50%	0.26	42.2
	C (medium vehicles)	Kia e-Niro	10%	0.28	64
	D (large vehicles)	Tesla Model 3 Long Range Performance	24%	0.27	75
	E+ (Executive and luxury vehicles)	Tesla Model X Long Range	16%	0.35	100

Top-oil temperature is defined as the average of the tank outlet oil temperature and the oil pocket temperature. The winding temperature is not uniform and the temperature of the hottest part of the winding is called hottest-spot temperature. The ultimate top-oil temperature rise over ambient temperature ($\Delta\theta_{UTO}^{t}$) and the ultimate winding hottest-spot temperature rise over top-oil temperature ($\Delta\theta_{UHS}^{t}$) at time *t* are obtained as

$$\Delta\theta_{UTO}^{t} = \Delta\theta_{RTO} \times \left(\frac{P_{LL}+P_{NLL}}{P_{LL-R}+P_{NLL}}\right)^{n}, \quad (9)$$

$$\Delta\theta_{UHS}^{t} = \Delta\theta_{\mathrm{RHS}} \times \left(\frac{P_{LL}}{P_{LL-R}}\right)^{m}, \quad (10)$$

where m and n are empirical values and depend on the cooling type of transformer. The cooling system of the transformers in this is oil natural air natural (ONAN), which is common in distribution networks. Under the steady-state condition, $\Delta\theta_{\mathrm{UTO}}^{t} = \Delta\theta_{TO}^{t}$ and $\Delta\theta_{\mathrm{UHS}}^{t} = \Delta\theta_{HS}^{t}$. Due to the continuous change of the transformer load and ambient temperature, $\Delta\theta_{TO}^{t}$ and $\Delta\theta_{HS}^{t}$ change before reaching the steady-state condition. Thus, the transient solution employs to obtain the top-oil rise over the ambient temperature ($\Delta\theta_{\mathrm{TO}}^{t}$) and the winding hottest-spot rise over the top-oil temperature ($\Delta\theta_{HS}^{t}$)

$$\Delta\theta_{TO}^{t} = \Delta\theta_{TO}^{t-1} + (\Delta\theta_{UTO}^{t} - \Delta\theta_{TO}^{t-1}) \times \left(1 - e^{-\frac{1}{\tau_{mTO}}}\right), \quad (11)$$

$$\Delta\theta_{HS}^{t} = \Delta\theta_{HS}^{t-1} + (\Delta\theta_{UHS}^{t} - \Delta\theta_{HS}^{t-1}) \times \left(1 - e^{-\frac{1}{\tau_{H}}}\right), \quad (12)$$

τ_{mTO} is the modified top-oil time constant which is expressed as

$$\tau_{mTO} = \tau_{TO} \times \frac{\left(\frac{\Delta\theta_{\mathrm{UTO}}^{t}}{\Delta\theta_{\mathrm{RTO}}}\right) - \left(\frac{\Delta\theta_{\mathrm{TO}}^{t-1}}{\Delta\theta_{\mathrm{RTO}}}\right)}{\left(\frac{\Delta\theta_{\mathrm{UTO}}^{t}}{\Delta\theta_{\mathrm{RTO}}}\right)^{\frac{1}{n}} - \left(\frac{\Delta\theta_{\mathrm{TO}}^{t-1}}{\Delta\theta_{\mathrm{RTO}}}\right)^{\frac{1}{n}}}. \quad (13)$$

According to (14), the winding hottest-spot temperature (θ_{HS}^{t}) is calculated as

$$\theta_{HS}^{t} = \Delta\theta_{HS}^{t} + \Delta\theta_{\mathrm{TO}}^{t} + TMP_{t}. \quad (14)$$

Finally, the aging acceleration factor of distribution transformer (F_a^t) is given as

$$F_a^t = \exp\left(\frac{15000}{383} - \frac{15000}{\theta_{HS}^{t}+273}\right). \quad (15)$$

The aging acceleration factor (F_a^t) is the rate that transformer insulation aging is accelerated compared to the aging rate at a reference hottest-spot temperature. If θ_{HS}^{t} exceeds the reference hottest-spot temperature, F_a^t will be greater than 1. Equation (16) is used to estimate the daily aging acceleration factor of the distribution transformer.

$$F_a^{daily} = \frac{\sum_{t=1}^{N_t} F_a^n \times \Delta t}{\sum_{t=1}^{N_t} \Delta t}, \quad (16)$$

where Δt is the simulation time step and considered 15 min in this paper.

Transformer loss of life (LoL) is the equivalent aging in hours at the reference hottest-spot temperature over a time period (usually 24h) which can be calculated as follows

$$LoL = F_a^{daily} \times 24. \quad (17)$$

The winding hottest-spot temperature is the most critical parameter in determining the transformer LoL. On the other hand, thermal stress obviously affects the winding hottest-spot temperature. Consequently, the transformer LoL depends on the thermal stress which is related to the transformer loading.

The thermal data of used transformers in this paper are tabulated in Table IV.

TABLE IV
THE TRANSFORMERS THERMAL DATA

$\Delta\theta_{\mathrm{RTO}}$ (°C)	$\Delta\theta_{\mathrm{RHS}}$ (°C)	n	m	τ_{TO} (min)	τ_{H} (min)
55	25	1	1.6	180	48

The total ownership cost (*TOC*) method can indicate the economic value of transformers. The purchase and losses costs of transformers are considered in this method. According to [19], *TOC* is formulated as

$$TOC = Pri + A \times P_{NLL} + B \times P_{LL}, \quad (18)$$

where A and B are capitalized parameters which multiply by losses to convert losses cost to the moment of purchase. These parameters depend on the expected transformer lifetime

(L_{Trans}), energy cost, and transformer loading. A and B are calculated according to (19) and (20)

$$A = 365 \times \frac{1-(\frac{1}{1+r})^{L_{Trans}}}{r} \times \sum_{t=1}^{24} \pi_t, \quad (19)$$

$$B = 365 \times \frac{1-(\frac{1}{1+r})^{L_{Trans}}}{r} \times \sum_{t=1}^{24} \pi_t \times (\frac{(p_t^{trans})^2+(q_t^{trans})^2}{(S_{rated}^{trans})^2}), \quad (20)$$

where L_{Trans} is defined as

$$L_{Trans} = \frac{DL}{F_a^{daily}}. \quad (21)$$

Using (18) the daily economic cost of transformer is calculated as

$$DOC = \frac{((1+r)^{1/365}-1)\times(1+r)^{L_{Trans}}}{((1+r)^{L_{Trans}}-1)\times(1+r)^{1/365}} \times TOC. \quad (22)$$

IV. Proposed Optimization Algorithm

In this section, the proposed algorithm is described in detail. The objective function and constraints of the proposed algorithm are presented and discussed. The objective function consists of two parts, energy losses (system-level) and transformers operating cost (equipment-level). The objective function is written as

$$OF = \min \left\{ \underbrace{DOC}_{\substack{\Downarrow \\ transformers\ cost}} + \underbrace{DLC}_{\substack{\Downarrow \\ energy\ losses\ cost}} \right\}, \quad (23)$$

subject to:

$$P_t^x = \sum_{y\epsilon N} V_t^x \times V_t^y \times Y_{xy} \times \cos(\theta_{xy} - \delta_t^x + \delta_t^y) \ \forall x \epsilon N, \quad (24)$$

$$Q_t^x = \sum_{y\epsilon N} V_t^x \times V_t^y \times Y_{xy} \times \sin(\theta_{xy} - \delta_t^x + \delta_t^y) \ \forall x \epsilon N, \quad (25)$$

$$p_t^x + jq_t^x = S_t^{load,x} + S_t^{Parking\ lot,x} \quad \forall x \epsilon N, \quad (26)$$

$$\sum_{t=1}^{T_p^n} \sum_{c=1}^{C_p^n} pve_t^{c,n} \times \Delta t = E_n^{G2V} \quad , n = 1, \dots, N_P, \quad (27)$$

$$SoC_t^{c,n} \leq SOC_U \, , n = 1, \dots, N_P \ \& \ c = 1, \dots, C_p^n \ \& \ t \leq T_p^n, \quad (28)$$

$$SoC_t^{c,n} \geq SOC_L \, , n = 1, \dots, N_P \ \& \ c = 1, \dots, C_p^n \ \& \ t \leq T_p^n, \quad (29)$$

$$SoC_{T_p^n}^{c,n} = SOC_U \ , n = 1, \dots, N_P \ \& \ c = 1, \dots, C_p^n, \quad (30)$$

$$(pve_t^{c,n})^2 + (qve_t^{c,n})^2 \leq (S_{rated,c})^2, \quad (31)$$

$$V_L \leq V_t^x \leq V_U, \quad (32)$$

$$\theta_{HS}^t \leq 120°C, \quad (33)$$

$$\frac{\sqrt{(p_t^{trans})^2+(q_t^{trans})^2}}{S_{rated}^{trans}} \leq 1.5. \quad (34)$$

DLC is the daily cost of energy losses which is calculated as follows

$$DLC = \sum_{t=1}^{N_t} \pi_t \times E_t^{loss}. \quad (35)$$

Constraints (24)-(26) are load flow equations. p_t^x and q_t^x are the injected active and reactive powers at node *x* of the grid and time *t* which are calculated by (26). Equation (26) expresses that in a node in which a parking lot is located, the apparent power of the node is the sum of the apparent power of the parking lot and other loads on the node. Constraint (27) indicates that the total electrical energy consumption and production of PEVs during their appearance in a parking lot equals the total energy needed for the parking lot (E_n^{G2V}). According to (28) and (29), PEV's SoC should not exceed SOC_U and should not fall short of SOC_L, respectively. Constraint (30) guarantees that PEVs will be fully charged when leaving parking lots. Constraint (31) is related to the operating curve of PEVs, which was described in detail in section III. B. According to the selected charging level, $S_{rated,c}$ is equal to 7.4 kW. Constraint (32) represents that the voltage of buses, which parking lots are connected to them, should be between V_L and V_U during the charging time. In this paper, V_L and V_U are selected 0.95 and 1.05 p.u., respectively. Constraints (33) and (34) are related to the operating limits of transformers. The maximum permitted hottest-spot temperature of transformers is $120°C$ and the loading of transformers beyond the nameplate rating is limited to 50% under normal cyclic loading conditions by IEC 60076-7 standard [32], [33]. According to (33) and (34), the hottest-spot temperature and loading of transformers should not exceed the maximum allowed values.

The pseudo-code of the proposed algorithm is shown in Algorithm 1. The aim is managing the values of $pve_t^{c,n}$ and $qve_t^{c,n}$ such that (23) is minimized. The variables are continuous. Due to the non-linear objective function and some non-linear constraints, non-linear programming (NLP) solver must be used. The interior-point optimization approach is adopted to minimize the objective function due to the superior performance compared to heuristic optimization approaches.

The proposed algorithm can be implemented on each distribution network. For this purpose, the bidirectional communication infrastructure is necessary to communicate the aggregator and parking lots with each other. At the first stage, the aggregator assembles data including the forecasted electricity price of next day from the independent system operator (ISO), the forecasted ambient temperature of next day from the meteorological center, the forecasted load profiles of next day for each bus and transformers data from the distribution company, and arrival and departure time, initial SoC, and type of PEVs from parking lots. The aggregator's estimator, using today and historical data, predicts the required data for the day-ahead scheduling. Afterward, the proposed co-optimization algorithm is carried out to schedule charging PEVs for the next day. Finally, the aggregator sends the managed charging strategy to parking lots. The fully charged

constraint (constraint (30)) cannot be met for some PEVs as a result of staying in parking lots for a limited time or very low level of SoC. Only PEVs, which mathematically have a potential for meeting the fully charged constraint, incorporate in the proposed algorithm. For this purpose, the estimated duration of stay for each PEV ($Time_{est}^{c,n}$) is requested from the PEV owner and the needed time ($Time_{needed}^{c,n}$) to fully charge up the PEV is calculated. If $Time_{est}^{c,n} \geq Time_{needed}^{c,n}$, the PEV incorporates in the proposed algorithm. Otherwise, the PEV must be charged with a constant charging rate which is 7.4kW in this paper.

Algorithm 1 The proposed algorithm

Require: PEVs characteristics, the forecasted ambient temperature, and electricity price.

1: **for** each parking lot $n \epsilon N_P$
2: **for** each PEV $c \epsilon C_p^n$
3: $E_n^{G2V} \leftarrow E_n^{G2V} + (SOC_U - SoC_0^{c,n}) \times BC$
4: $Time_{needed}^{c,n} \leftarrow \frac{(SOC_U - SoC_0^{c,n}) \times BC}{7.4}$
5: **if** $Time_{est}^{c,n} \geq Time_{needed}^{c,n}$
6: Go to line 12
7: **else**
8: Charge up with 7.4 kW
9: **end**
10: **end**
11: **end**
12: Generating an initial point
13: **While** $|OF_{\ell+1} - OF_{\ell}| > \varepsilon$
14: **for** each iteration
15: Updating p_t^x and q_t^x using (26)
16: **for** each time step $t \epsilon T_p^n$
17: Performing power flow
18: Obtaining F_a^t using (15)
19: $F_a^{daily} \leftarrow F_a^{daily} + \frac{F_a^t \times \Delta t}{\sum_{n=1}^{T_p^n} \Delta t}$
20: $DLC \leftarrow DLC + \pi_t \times E_t^{loss}$
21: **end**
22: Calculating DOC using (22)
23: $OF_{\ell+1} \leftarrow DOC + DLC$
24: Updating $pve_t^{c,n}$ and $qve_t^{c,n}$
25: **end**
26: **end**

V. Simulation Results

In this section, the proposed algorithm is implemented in the feeder of Sirjan city center's distribution network to evaluate it. Fig. 4 illustrates the benchmark system. More details about the case study can be studied in [34]. It is assumed that three parking lots are located in the commercial workplace with a capacity of 80, 80, and 240 vehicles. According to section III, the stochastic characteristics of PEVs, e.g., arrival and departure times and vehicle types, are determined. Real-time pricing is extracted from [35]. The features of the transformers are shown in Table V [36]. P_{ohm}, P_{EC}, and P_{OSL} are calculated according to the value of P_{LL} based on a method which is introduced in [37]. The transformer purchase price is 166.1 \$/kVA [17]. The harmonic current content of PEV chargers is tabulated in Table VI [38]. The simulations are conducted for a typical spring weekday in MATLAB R2019a and the interior-point method is employed to solve the optimization problems.

The case study is scrutinized under four scenarios. The scenarios are as follows

- **Base scenario**: Uncoordinated charging of PEVs.
- **Scenario 1**: Managing the active power of PEVs based on minimizing energy losses cost.
- **Scenario 2**: Managing the active power of PEVs based on minimizing DOC of transformers.
- **Scenario 3**: Managing the active power of PEVs based on minimizing (23).
- **Scenario 4**: Managing both active and reactive powers of PEVs based on minimizing (23).

TABLE V
THE TRANSFORMERS FEATURES

Transformer	Nominal size (kVA)	P_{NLL} (kW)	P_{LL} (kW)
Parking lot no.1 (with 80 capacity)	315	1.05	4.2
Parking lot no.2 (with 80 capacity)	315	1.05	4.2
Parking lot no.3 (with 240 capacity)	500	0.73	5.5

TABLE VI
HARMONIC CURRENT CONTENT OF PEV CHARGERS [38]

Harmonic order	Magnitude (%)	Angle (°)
1	100	-26
5	25	-94
7	17	-67
11	9	-67
13	5	-46

The simulation results are summarized in Table VII. Scenario 1, which minimizes energy losses cost, has the most value of F_a^{daily}. Moreover, scenario 2, which minimizes *DOC*, has most energy losses and energy losses cost values. These illustrate that it is necessary to minimize the total daily operating cost. Using scenario 3, the objective function improves 5.98% compared with that of the base scenario. As mentioned earlier, reactive power plays a crucial role in the improvement of daily aging acceleration factor and energy losses. For this reason, both active and reactive powers are managed in scenario 4 in order to minimize the total daily operating cost of the distribution network. The objective function using scenario 4 gets better 11.81% compared to the base scenario. *DOC* and energy losses cost of scenario 4 are improved by 2.08% and 7.07%, respectively compared to that of scenario 3. The first effect of the reactive power compensation is the reduction of energy losses and transformers loading. Reducing the loading of the transformers makes it possible for PEVs to get more charge in some hours. The fact that PEVs get more charge causes raising *DOC*. For this reason, the improvement in *DOC* is less than the energy losses cost. Eventually, according to Table VII, it is proven that scenario 4 is the best scenario for minimizing the total daily operating cost of the grid. On the other hand, the benefit of PEVs owners is important. In the real-time pricing method, electricity tariff changes during the day in a way that

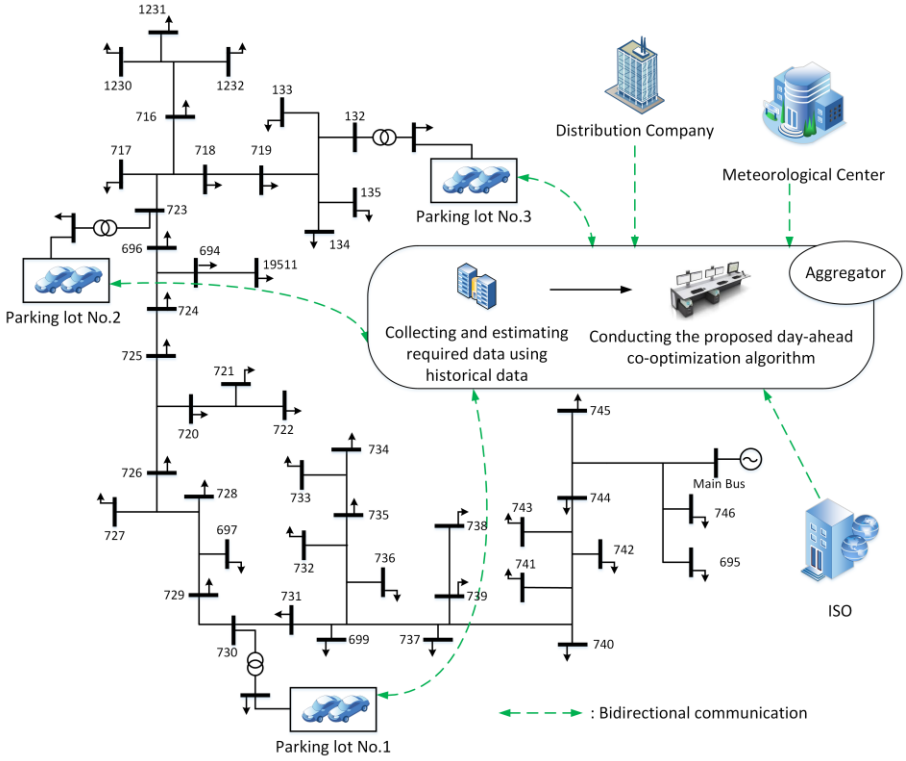

Fig. 4. The distribution network under study.

TABLE VII
THE RESULTS OF DIFFERENT SCENARIOS

Scenario	Energy losses (MWh)	Energy losses cost ($)	F_a^{daily}	DOC ($)	Charging cost ($)	Objective function ($)
Base	1.02	809.74	3.7	283.92	1918.45	1093.66
1	1.01	797.49	0.89	234.92	1625.97	1032.41
2	1.01	804.41	0.75	223.81	1870.47	1028.22
3	1.01	800.33	0.75	225.47	1771.05	1025.8
4	0.93	743.73	0.65	220.77	1734.78	964.5

the electricity price is high during peak times. In other words, tariff and load profiles have almost the same trend. In addition, to minimize the energy losses cost, the proposed algorithm schedules charging PEVs in a way that PEVs are charged during off-peak times (when the tariff is low) and discharged during peak times (when the tariff is high). This means that the proposed algorithm also reduces the charging cost of PEVs by reducing the energy losses cost. In Table VII, scenario 1 has the lowest charging cost, and scenario 2 has the highest charging cost.

The active power and hottest-spot temperature of transformers illustrate for all parking lots in Fig. 5 and Fig. 6, respectively. The results are analyzed for parking lot no.1 as below.

From 7:00 am to 8:30 am, both power consumption and the electricity tariff are medium. Thus, if PEVs are charged in these conditions, the energy losses cost will be decreased. Besides, charging PEVs reduces *DOC* because the ambient and hottest-spot temperature are low in this period. Therefore, all of the scenarios suggest that PEVs are charged in this period.

From 8:30 am to 12:00 pm, the power consumption is high and the ambient and hottest-spot temperature rise. So, in order to minimize the energy losses cost and *DOC*, PEVs must be discharged in all scenarios except scenario 2. PEVs in scenario 1 are discharged more than other scenarios because it tends to steady the load profile. On the other hand, PEVs in scenario 2 are not charged because of the high loading and hottest-spot temperature of the transformer. Also, PEVs in scenario 2 are not discharged because discharging PEVs increase the power consumption of next hours and as a result gain *DOC*.

From 12:00 pm to 6:15 pm, PEVs in Scenarios 1, 3, and 4 are charged because they try to steady the load curve to minimize energy loss. Note that scenario 4 can compensate for reactive power so that it can reduce as well as *DOC* of the transformer. In scenario 2, although the ambient temperature is high, the PEVs are charged because the loading and hottest-spot temperature of the transformer are low in this period. Due to the reactive power injection and reducing the loading of the transformer, the transformer has the lowest hottest-spot temperature in scenario 4.

Fig. 7a and Fig. 7b show the active and reactive power of the whole distribution network. It can be seen that the peak value and peak time of the load profile change from 3.73 MW at 8:00 pm to 4.2 MW at 8:15 am in the base scenario, respectively. In other words, the uncoordinated charging of PEVs causes the appearance of a new large morning peak. The weighted standard deviation equals 86.67 for the load profile of scenario 1 that is the lowest value compared to the other scenarios. It illustrates that as mentioned earlier, the load profile for scenario 1 is smoother than the other scenarios. Fig. 7a demonstrates that

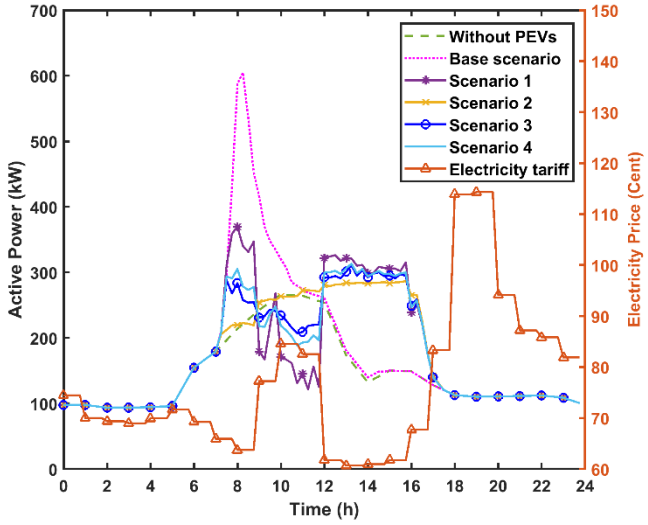

(a)

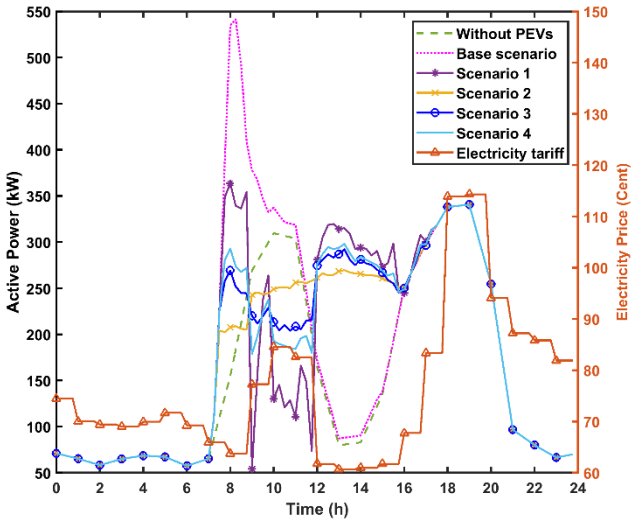

(b)

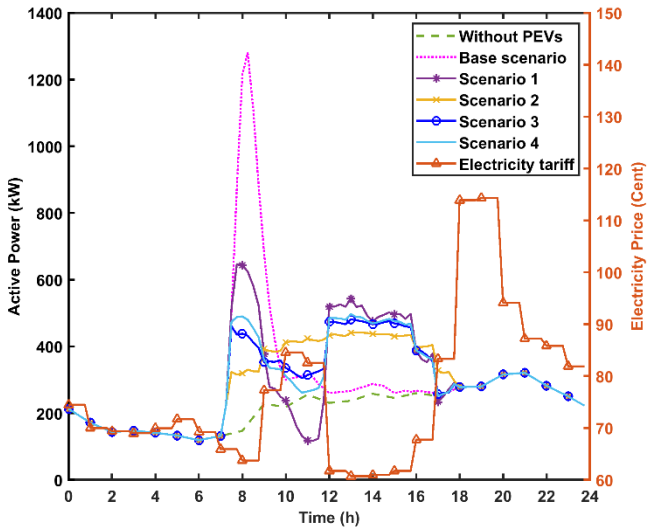

(c)

Fig. 5. The active power of transformers and electricity price for (a) parking lot no.1. (b) parking lot no.2. (c) parking lot no.3.

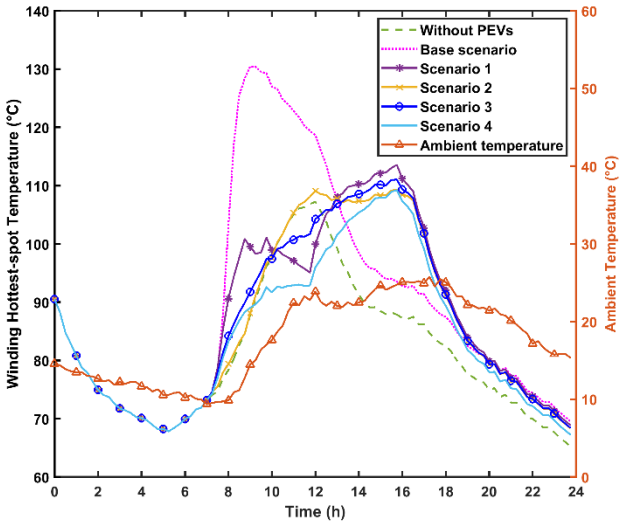

(a)

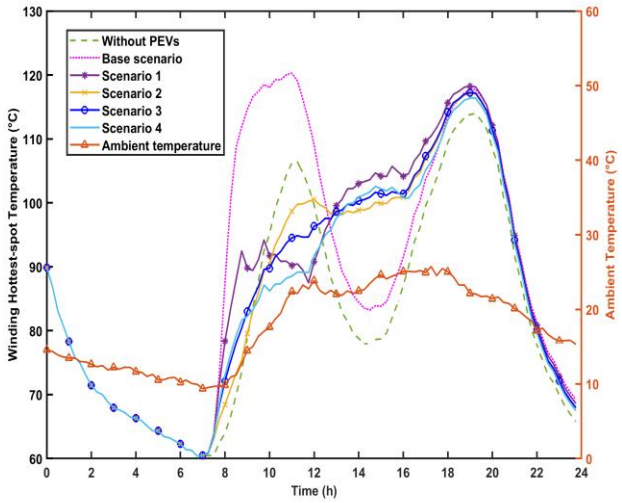

(b)

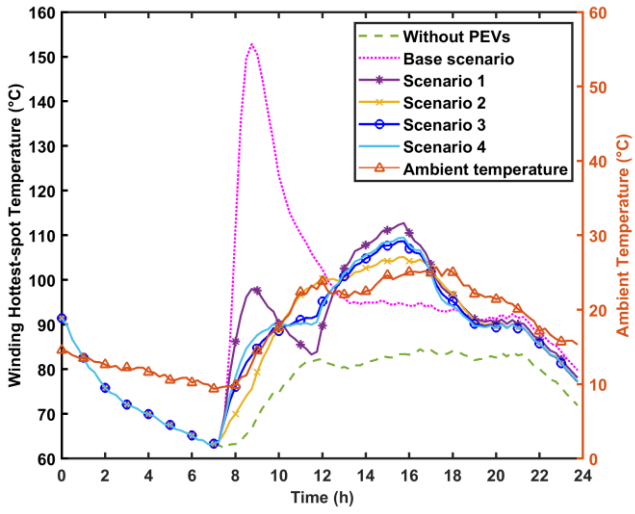

(c)

Fig. 6. The winding hottest-spot temperature of transformers and the ambient temperature for (a) parking lot no.1. (b) parking lot no.2. (c) parking lot no.3.

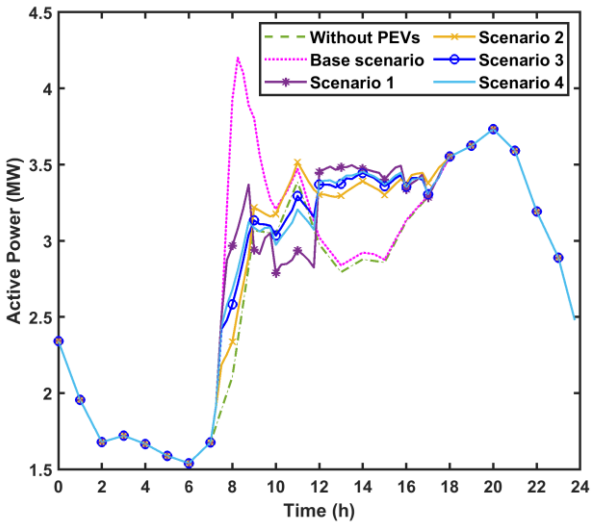

(a)

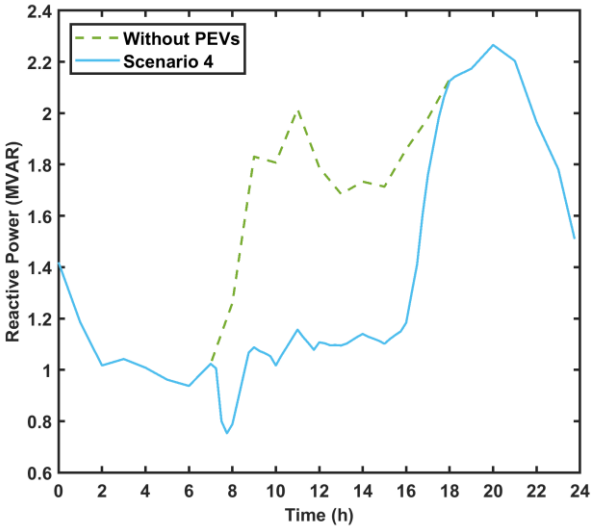

(b)

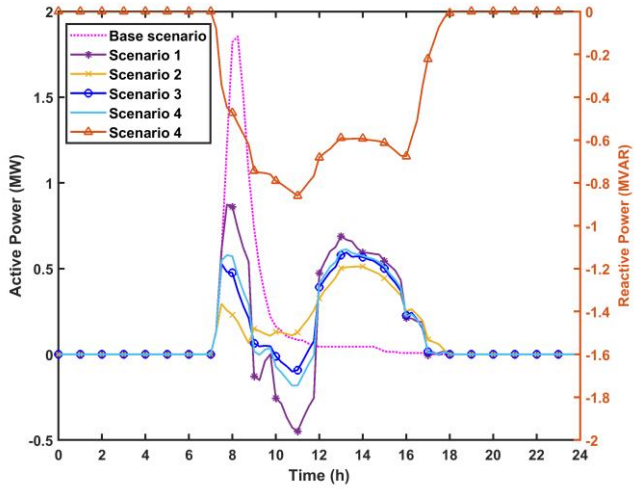

(c)

Fig. 7. (a) the active power curve of the grid. (b) the reactive power curve of the grid (c) the contribution of PEVs under the proposed scenarios.

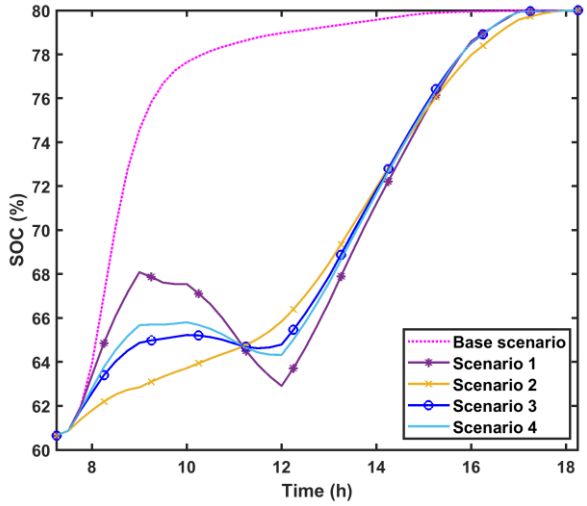

Fig. 8. The average SoC of PEVs during the charging process.

scenario 2 tends to charge PEVs when either the temperature or the loading of transformers is low. For this reason, the load profile of scenario 2 has the most magnificent peak quantity among scenarios 1 to 4 (3.6 MW). There was a trade-off between energy losses cost and *TOC* minimizing if the total daily cost is wanted to minimize. Therefore, the load profile for scenario 3 is between scenario 1 and 2 load profiles. Similar to scenario 3, scenario 4 tries to minimize the total daily cost by managing PEV's active and reactive powers simultaneously. The reactive power injection decreases the loading of the transformers and as a result, decreases hottest-spot temperature. Therefore, the reactive power compensation causes that PEVs get more charge when the ambient temperature is high. For this reason, in scenario 4, the discharge of PEVs increases during peak times compared with that in scenario 3. This increase in the discharge of PEVs reduces energy losses and charging costs because PEVs sell the active power when the electricity price is high and buy active power when the electricity price is lower. As seen in Fig. 7, in scenario 4, the peak value of the load profile is equal to the peak value of the load profile when PEVs are not connected to the grid. It means that managing the charging of PEVs by scenario 4 does not affect the infrastructures of the power system. Fig. 7b shows that a big change is occurred in reactive power after 4 pm. This big change causes some transient effects on the grid which are not considered in this paper.

Fig. 8 shows the average SoC of PEVs during the charging process under different scenarios. As expected, the SoC of PEVs continuously increases in the base scenario. The most of PEVs are fully charged in the early hours in a way that the average SoC of PEVs is almost 77.27% at 9:45 am. Among the proposed scenarios, PEVs in scenario 1 have the most fluctuation in their SoC because PEVs are discharged in scenario 1 more than other scenarios. Also, PEVs in scenario 2 have the least fluctuation in their SoC because PEVs in scenario 2 are not almost discharged and are continuously charged. As seen in Fig. 8, all of the scenarios satisfy constraints (28)-(30).

Decreasing the total daily cost is not the sole effect of reactive power management on the grid. The reactive power injection improves the grid power factor that is shown in Fig. 9.

TABLE VIII
THE RESULTS OF THE SENSITIVITY ANALYSIS ON THE NUMBER OF PEVS

The total number of PEVs	Scenario	Energy losses (MWh)	Energy losses cost ($)	F_a^{daily}	DOC ($)	Charging cost ($)	Objective function ($)
500	Base	1.09	825.58	22.93	516.86	2271.29	1342.44
	4	0.94	755.48	0.83	228.48	2143.14	983.96
400	Base	1.02	809.74	3.7	283.92	1918.45	1093.66
	4	0.93	743.73	0.65	220.77	1734.78	964.5
300	Base	0.99	789.99	1.09	236.69	1358.04	1026.68
	4	0.91	730	0.48	207.32	1213.05	937.32
200	Base	0.97	777.57	0.68	217.16	1011.53	994.73
	4	0.89	720.8	0.42	200.47	845.83	821.27

TABLE IX
THE RESULTS OF THE SENSITIVITY ANALYSIS ON DISTRIBUTIONS OF PEVS

Change in distributions of PEVs	Scenario	Energy losses (MWh)	Energy losses cost ($)	F_a^{daily}	DOC ($)	Charging cost ($)	Objective function ($)
+10% segments 1 and 2	Base	1.01	807.01	3.07	274.78	1842.84	1081.79
-10% segments 3 and 4	4	0.93	743.95	0.63	217.35	1703.55	961.3
+5% segments 1 and 2	Base	1.01	807.49	3.27	277.62	1854.03	1085.11
-5% segments 3 and 4	4	0.93	744.22	0.62	217.27	1712.48	961.49
Without change	Base	1.02	809.74	3.7	283.92	1918.45	1093.66
	4	0.93	743.73	0.65	220.77	1734.78	964.5
-5% segments 1 and 2	Base	1.01	809.05	3.94	286.61	1883.47	1095.64
+5% segments 3 and 4	4	0.93	743.49	0.67	221.12	1734.86	964.61
-10% segments 1 and 2	Base	1.01	808.75	5.42	305.82	1855.49	1114.57
+10% segments 3 and 4	4	0.93	743.11	0.73	221.78	1713.57	964.89

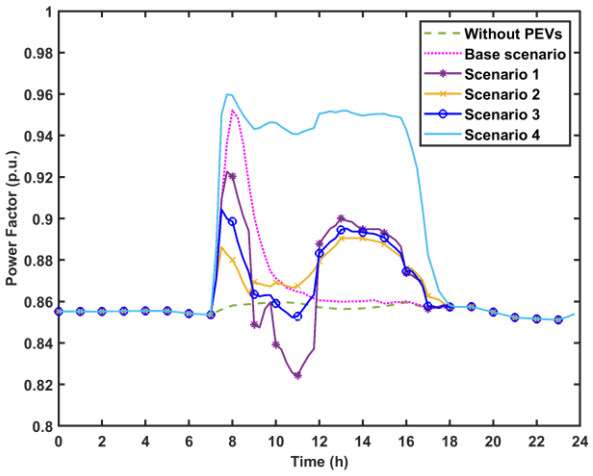

Fig. 9. The power factor of the grid under various scenarios for the whole day.

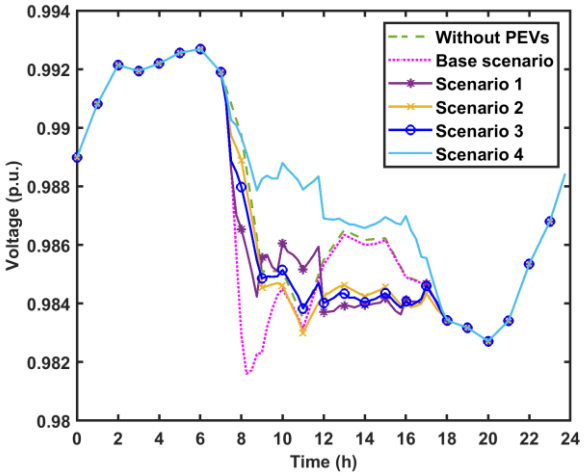

(a)

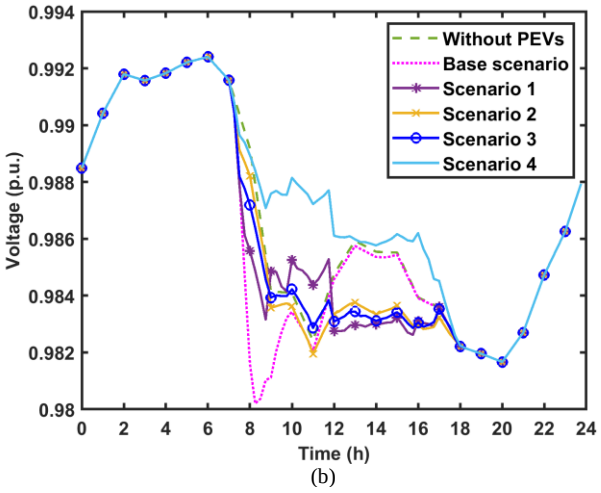

(b)

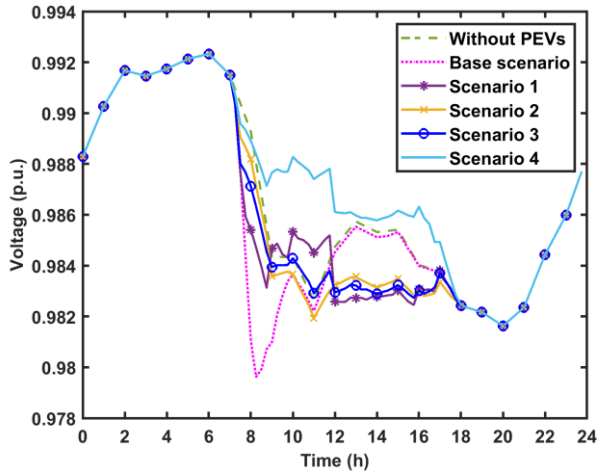

(c)

Fig. 10. The voltage profiles of the scenarios for (a) parking lot no.1. (b) parking lot no.2. (c) parking lot no.3.

The average power factor during the charging time enhances from 0.86 (without PEV) to 0.93 (in scenario 4). Scenario 1 has a point with the minimum power factor (0.82) among all scenarios because of the huge discharging of PEVs in the said point. Further, the management of reactive power can enhance the voltage of buses that parking lots are connected to them. The average voltage of the buses, shown in Fig. 10, improves from 0.985, 0.984, and 0.984 in the base scenario to 0.987, 0.987, and 0.987 in scenario 4 during the charging time.

To assess the robustness of the proposed algorithm, a sensitivity analysis is performed on the number and distributions of PEVs. The sensitivity analysis can clarify the effects of changing the number and distributions of PEVs on the charging strategy. The results of changing the number and distributions of PEVs are tabulated in Table VIII and Table IX, respectively. In a case that the number of PEVs is 500, 80.45% of the improvement of the objective function is related to the improvement of *DOC* while when the number of PEVs is 200, the share of the improvement of *DOC* in the improvement of the objective function is 9.62%. This means that by increasing the number of PEVs, the daily operating cost of transformers plays a more important role in the proposed algorithm.

VI. CONCLUSION

Environmental issues have been a motivation to use PEVs. Even though PEVs have many advantages, they can have undesirable impacts on grids. This paper proposed a co-optimization algorithm to mitigate the effects of PEVs on distribution networks. The proposed day-ahead algorithm concentrated on minimizing the cost of energy losses alongside the transformer operating cost in the presence of harmonics using the management of PEVs active and reactive power. The temperature and the PEV owners' behaviors were modeled stochastically. TOC method was employed to calculate the transformers operating cost because in this method, in addition to the purchase price of transformers, the losses cost and the loading of them are involved. One strength of this paper is that it was implemented on the real distribution network to validate the proposed algorithm. The optimization problem was solved by the interior-point method. The findings indicated that the proposed algorithm declined the total daily cost of the grid 11.81% in contrast with the uncoordinated charging. The proposed algorithm did not significantly alter the peak value of the load profile. Therefore, using the proposed algorithm, PEVs charging did not impact on the infrastructure of the power system. One of the more significant findings to emerge from this paper was that reactive power compensation enhanced the power quality parameters such as voltage and power factor. The average power factor during the charging time improved by 8.9%, compared to that of the base scenario. Furthermore, the average voltage of the buses of the parking lots during the charging time improved by about 0.26%, in contrast to that of the uncoordinated charging of PEVs. Also, the robustness of the algorithm was shown by changing the number and distribution of PEVs.

REFERENCES

[1] "World of Change: Global Temperatures." [Online]. Available: https://earthobservatory.nasa.gov/world-of-change/global-temperatures.

[2] E. Akbostancı, G. İ. Tunç, and S. Türüt-Aşık, "Drivers of fuel based carbon dioxide emissions: The case of Turkey," *Renew. Sustain. Energy Rev.*, vol. 81, no. June 2017, pp. 2599–2608, 2018.

[3] R. Mehta, P. Verma, D. Srinivasan, and J. Yang, "Double-layered intelligent energy management for optimal integration of plug-in electric vehicles into distribution systems," *Appl. Energy*, vol. 233–234, no. April 2018, pp. 146–155, 2019.

[4] S. S. Raghavan and A. Khaligh, "Electrification potential factor: Energy-based value proposition analysis of plug-in hybrid electric vehicles," *IEEE Trans. Veh. Technol.*, vol. 61, no. 3, pp. 1052–1059, 2012.

[5] M. D. and E. Knipping, "Environmental Assessment of PlugIn Hybrid Electric Vehicles," *EPR*, 2007.

[6] D. Wu, H. Zeng, C. Lu, and B. Boulet, "Two-Stage Energy Management for Office Buildings with Workplace EV Charging and Renewable Energy," *IEEE Trans. Transp. Electrif.*, vol. 3, no. 1, pp. 225–237, 2017.

[7] S. M. Kandil, H. E. Z. Farag, M. F. Shaaban, and M. Z. El-Sharafy, "A combined resource allocation framework for PEVs charging stations, renewable energy resources and distributed energy storage systems," *Energy*, vol. 143, pp. 961–972, 2018.

[8] L. Calearo, A. Thingvad, K. Suzuki, and M. Marinelli, "Grid Loading Due to EV Charging Profiles Based on Pseudo-Real Driving Pattern and User Behavior," *IEEE Trans. Transp. Electrif.*, vol. 5, no. 3, pp. 683–694, 2019.

[9] M. Muratori, "Impact of uncoordinated plug-in electric vehicle charging on residential power demand," *Nat. Energy*, vol. 3, no. 3, pp. 193–201, 2018.

[10] Z. Moghaddam, I. Ahmad, D. Habibi, and Q. V. Phung, "Smart Charging Strategy for Electric Vehicle Charging Stations," *IEEE Trans. Transp. Electrif.*, vol. 4, no. 1, pp. 76–88, 2017.

[11] M. F. Shaaban, Y. M. Atwa, and E. F. El-Saadany, "PEVs modeling and impacts mitigation in distribution networks," *IEEE Trans. Power Syst.*, vol. 28, no. 2, pp. 1122–1131, 2012.

[12] K. N. Kumar, S. Member, and B. Sivaneasan, "Impact of Priority Criteria on Electric Vehicle Charge Scheduling," vol. 1, no. 3, pp. 200–210, 2015.

[13] H. Nafisi, S. M. M. Agah, H. A. Abyaneh, and M. Abedi, "Two-Stage Optimization Method for Energy Loss Minimization in Microgrid Based on Smart Power Management Scheme of PHEVs," *IEEE Trans. Smart Grid*, vol. 7, no. 3, pp. 1268–1276, 2016.

[14] M. Moeini-Aghtaie, A. Abbaspour, and M. Fotuhi-Firuzabad, "Online multicriteria framework for charging management of PHEVs," *IEEE Trans. Veh. Technol.*, vol. 63, no. 7, pp. 3028–3037, 2014.

[15] S. Acha, T. C. Green, and N. Shah, "Effects of optimised plug-in hybrid vehicle charging strategies on electric distribution network losses," *2010 IEEE PES Transm. Distrib. Conf. Expo. Smart Solut. a Chang. World*, no. March 2014, 2010.

[16] E. Ramos Muñoz, G. Razeghi, L. Zhang, and F. Jabbari, "Electric vehicle charging algorithms for coordination of the grid and distribution transformer levels," *Energy*, vol. 113, pp. 930–942, 2016.

[17] M. R. Sarker, D. J. Olsen, and M. A. Ortega-Vazquez, "Co-Optimization of Distribution Transformer Aging and Energy Arbitrage Using Electric Vehicles," *IEEE Trans. Smart Grid*, vol. 8, no. 6, pp. 2712–2722, 2017.

[18] O. Beaude, S. Lasaulce, M. Hennebel, and I. Mohand-Kaci, "Reducing the Impact of EV Charging Operations on the Distribution Network," *IEEE Trans. Smart Grid*, vol. 7, no. 6, pp. 2666–2679, 2016.

[19] "Total Cost of Ownership method Basics of transformer TCO calculation," 2015. [Online]. Available: https://new.abb.com/docs/librariesprovider95/energy-efficiency-library/tco-method-basics.pdf?sfvrsn=2.

[20] M. H. Mobarak and J. Bauman, "Vehicle-Directed Smart Charging Strategies to Mitigate the Effect of Long-Range EV Charging on Distribution Transformer Aging," *IEEE Trans. Transp. Electrif.*, vol. 5, no. 4, pp. 1097–1111, 2019.

[21] V. Farahani, B. Vahidi, and H. A. Abyaneh, "Reconfiguration and capacitor placement simultaneously for energy loss reduction based on an improved reconfiguration method," *IEEE Trans. Power Syst.*, vol. 27, no. 2, pp. 587–595, 2012.

[22] C. Le Floch, F. Belletti, and S. Moura, "Optimal Charging of Electric Vehicles for Load Shaping: A Dual-Splitting Framework with

Explicit Convergence Bounds," *IEEE Trans. Transp. Electrif.*, vol. 2, no. 2, pp. 190–199, 2016.

[23] O. Olatujoye, F. J. Ardakani, A. J. Ardakani, and J. McCalley, "Co-optimization in power systems," in *2017 North American Power Symposium (NAPS)*, 2017, pp. 1–6.

[24] S. M. M. Agah and H. A. Abyaneh, "Quantification of the distribution transformer life extension value of distributed generation," *IEEE Trans. Power Deliv.*, vol. 26, no. 3, pp. 1820–1828, 2011.

[25] "National Household Travel Survey." [Online]. Available: https://nhts.ornl.gov/.

[26] S. Shafiee, M. Fotuhi-Firuzabad, and M. Rastegar, "Investigating the impacts of plug-in hybrid electric vehicles on power distribution systems," *IEEE Trans. Smart Grid*, vol. 4, no. 3, pp. 1351–1360, 2013.

[27] "Compare electric vehicles - EV Database." [Online]. Available: https://ev-database.org/.

[28] G. Chrysanidis, D. Kosmanos, A. Argyriou, and L. Maglaras, "Stochastic optimization of electric vehicle charging stations," *Proc. - 2019 IEEE SmartWorld, Ubiquitous Intell. Comput. Adv. Trust. Comput. Scalable Comput. Commun. Internet People Smart City Innov. SmartWorld/UIC/ATC/SCALCOM/IOP/SCI 2019*, pp. 1–7, 2019.

[29] X. Zhang, E. Gockenbach, V. Wasserberg, and H. Borsi, "Estimation of the Lifetime of the Electrical Components in Distribution Networks," vol. 22, no. 1, pp. 515–522, 2007.

[30] "IEEE Guide for Loading Mineral-Oil-Immersed Transformers," *IEEE Std C57.91-1995*. p. i, 1996.

[31] H. Turker, S. Bacha, D. Chatroux, and A. Hably, "Low-voltage transformer loss-of-life assessments for a high penetration of plug-in hybrid electric vehicles (PHEVs)," *IEEE Trans. Power Deliv.*, vol. 27, no. 3, pp. 1323–1331, 2012.

[32] Y. Gao, B. Patel, Q. Liu, Z. Wang, and G. Bryson, "Methodology to assess distribution transformer thermal capacity for uptake of low carbon technologies," *IET Gener. Transm. Distrib.*, vol. 11, no. 7, pp. 1645–1651, 2017.

[33] P. Transformers—Part, "7: loading guide for oil-immersed power transformers," *IEC Stand.*, vol. 60076, no. 7, 2005.

[34] V. Farahani, S. H. H. Sadeghi, H. A. Abyaneh, S. M. M. Agah, and K. Mazlumi, "Energy Loss Reduction by Conductor Replacement and Capacitor Placement in Distribution Systems," *IEEE Trans. Power Syst.*, vol. 28, no. 3, pp. 2077–2085, 2013.

[35] "Southern California Edison RTP." [Online]. Available: https://library.sce.com/content/dam/sce-doclib/public/regulatory/tariff/electric/schedules/general-service-&-industrial-rates/ELECTRIC_SCHEDULES_TOU-GS-1-RTP.pdf.

[36] "abb distribution transformer catalog." [Online]. Available: http://ocw.uniovi.es/pluginfile.php/5422/mod_resource/content/1/Catálogo transformadores ABB.pdf.

[37] E. Hajipour, M. Mohiti, N. Farzin, and M. Vakilian, "Optimal distribution transformer sizing in a harmonic involved load environment via dynamic programming technique," *Energy*, vol. 120, pp. 92–105, 2017.

[38] R. Misra, S. Paudyal, O. Ceylan, and P. Mandal, "Harmonic distortion minimization in power grids with wind and electric vehicles," *Energies*, vol. 10, no. 7, p. 932, 2017.

Seyed Soroush Karimi Madahi received the B.Sc. degree in electrical engineering from Amirkabir University of Technology, Tehran, Iran, in 2018. He is currently pursuing the Master of Electrical Engineering at Amirkabir University of Technology, Tehran, Iran. His current research interests include the smart charging of PEVs, islanding detection of distributed generations, and power system protection.

Hamed Nafisi received the B.Sc., M.Sc., and Ph.D. degrees in electrical engineering from the Iranian Center of Excellence in Power Systems, Amirkabir University of Technology, Tehran, Iran, in 2006, 2008, and 2014, respectively. He is currently an Assistant Professor with the Department of Electrical Engineering, Amirkabir University of Technology. His current research interests include smart grid, power system protection, and power electronics application in power systems.

Hossein Askarian Abyaneh received his B.S. degree from Iran University of Science and Technology in 1976 and M.S. degree from Tehran University, Tehran, Iran, in 1982, both in Electrical Engineering. He received a second M.S. degree and the Ph.D. degree, both in Power Engineering, from the University of Manchester Institute of Science and Technology, Manchester, U.K., in 1985 and 1988, respectively. Currently, he is a Professor with the Department of Electrical Engineering, Amirkabir University of Technology, Tehran, Iran. He has published numerous scientific papers in reviewed journals and presented at international conferences. His research interests include power system protection and power quality.

Mousa Marzband (SM'17) received the Ph.D. degree in electrical engineering from the Department of Electrical Engineering, Polytechnic University of Catalunia, Barcelona, Spain, in 2014. After his PhD, he joined the University of Manchester, Manchester, UK as a Post-Doctoral Research Fellow and then joined the University College Cork, Cork, Ireland, as a Senior Researcher. He is currently a Senior Lecture (Associate professor) with the Department of Match, Physics, Electrical Engineering, Northumbria University, Newcastle, UK. Due to the high numbers of citations for his research, he has recently been appointed as an honorary distinguished adjunct professor by King Abdulaziz University, Jeddah, Saudi Arabia (judged to be the best university in the Arab World by THE in 2019). The reason behind this is that he is highly Cited Researcher in 2019. He is nominated in 2018 and 2019 by Thomson Reuters to be the world's top 1% researchers in engineering. His research findings have been published in two books and more than 80 top field journals and over 40 proceedings of the international conferences. Recently, as a co-investigator, he helped to secure the UK-India grant (£185K), funded by Britich Council and started in May 2019, to develop the power electronics schemes for a smart micro grid with high penetration of PV generation and electric vehicles. His research interests include operation and control strategies in DGs, mathematical modelling and control of optimal energy management system within multi-energy carrier systems, and cooperative and non-cooperative game theory applications in energy market.